Discrete field of view sampling of satellite and ground-based DOAS-type instruments using high-resolution imager data

H. Sihler, S. Beirle, P. Lübcke, J. Remmers, and T. Wagner

MPIC, Mainz, Germany
IUP, Heidelberg, Germany

6th July 2015

Introduction
Comparison of SO_2-camera and NFOV-DOAS

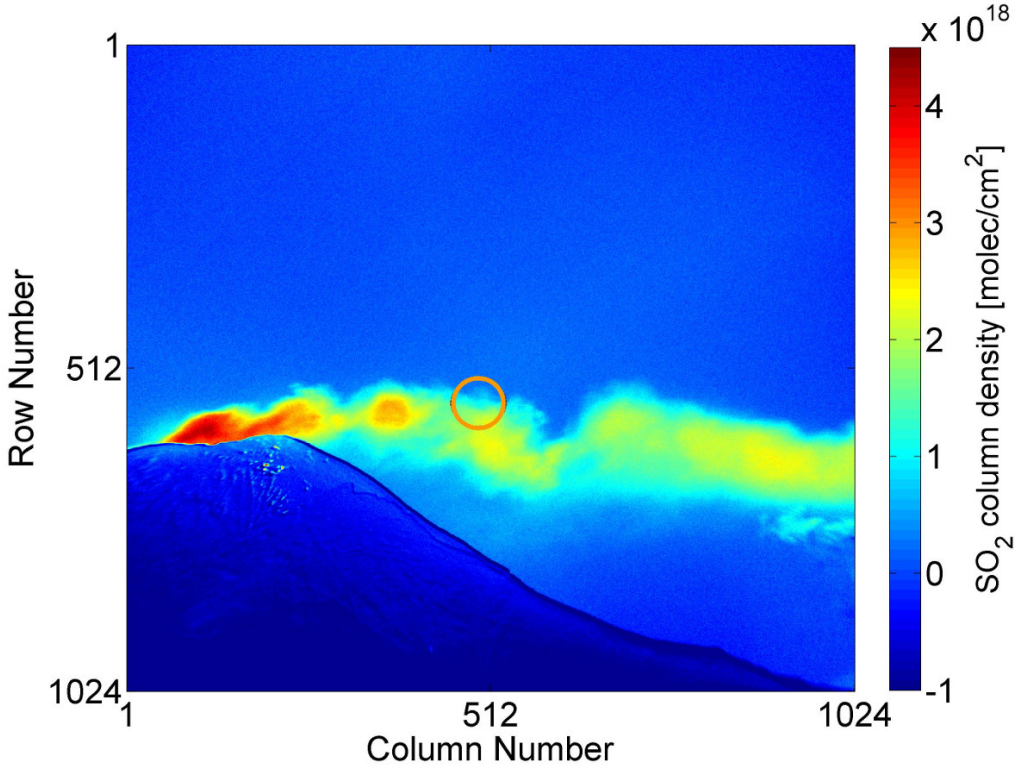

[P. Lübcke *et al.*, 2013]

- SO_2-camera image from Popocatépetl 1 March 2011,
- circular FOV from lab calibration
- telescope alignment changed during field deployment
- position of maximum correlation is FOV center

Introduction
Comparison of OMI and car MAX-DOAS

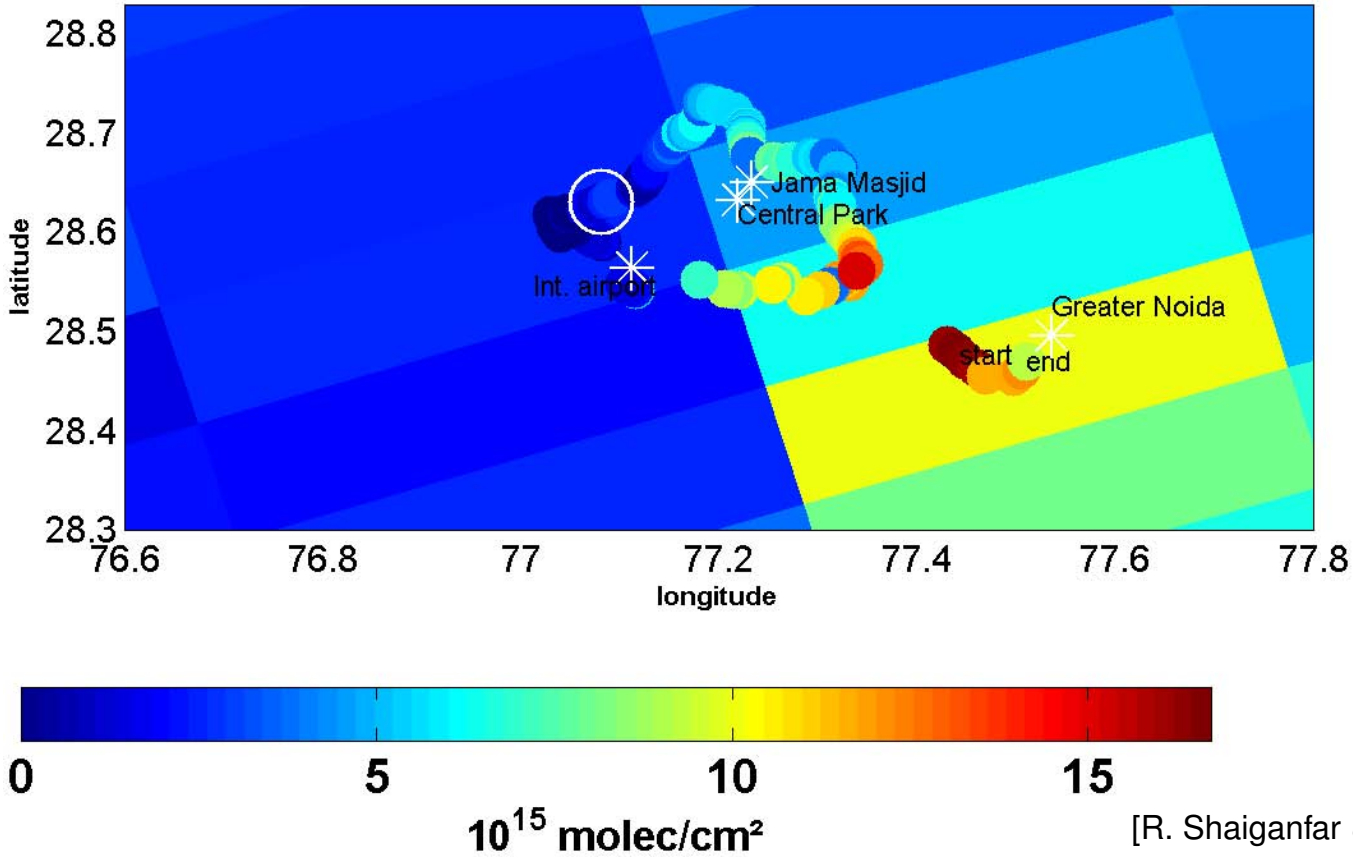

[R. Shaiganfar *et al.*, 2011]

- NO_2 VCDs Delhi 14 April 2010
- car MAX-DOAS provides higher spatial resolution

➔ spatial response of OMI?

Introduction

Improved OMI spatial interpolation by G. Kuhlmann *et al.*, 2014

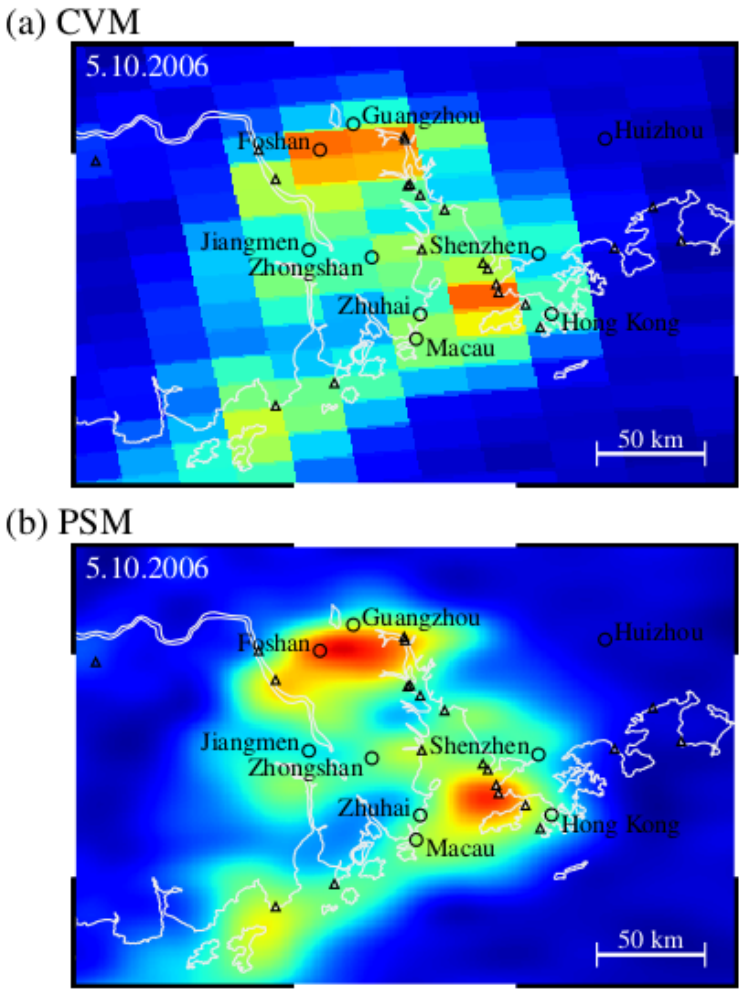

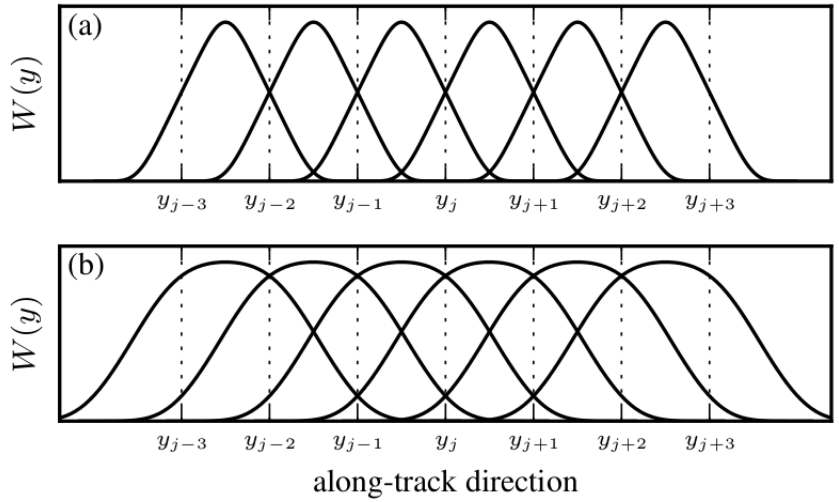

CVM constant value method

PSM parabolic spline method

Introduction

Spatial vs. spectral resolution

LR low *spatial* resolution, but high spectral resolution

HR high *spatial* resolution, but low spectral resolution

Goal

Infer LR field of view (FOV) from comparison with HR imager data!

Examples for LR/HR instrument pairs

LR	$\leftrightarrow$	HR
GOME-2		AVHRR
OMI		MODIS Aqua
NFOV-DOAS		SO_2-camera

Spectral range of GOME-2 vs. AVHRR

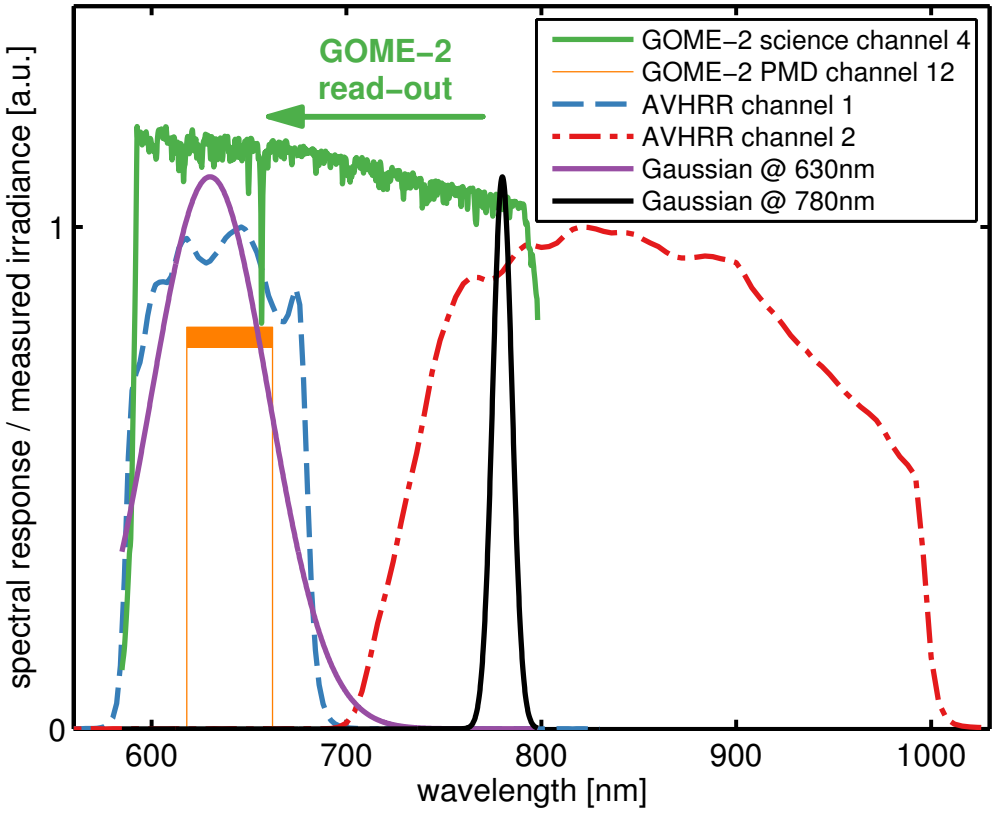

- GOME-2 channel 4 readout → spatial aliasing
- which LR convolution kernels / AVHRR channel?
- LR/HR correlation is reduced by red-edge (≈700 nm)

Method
Data regularization

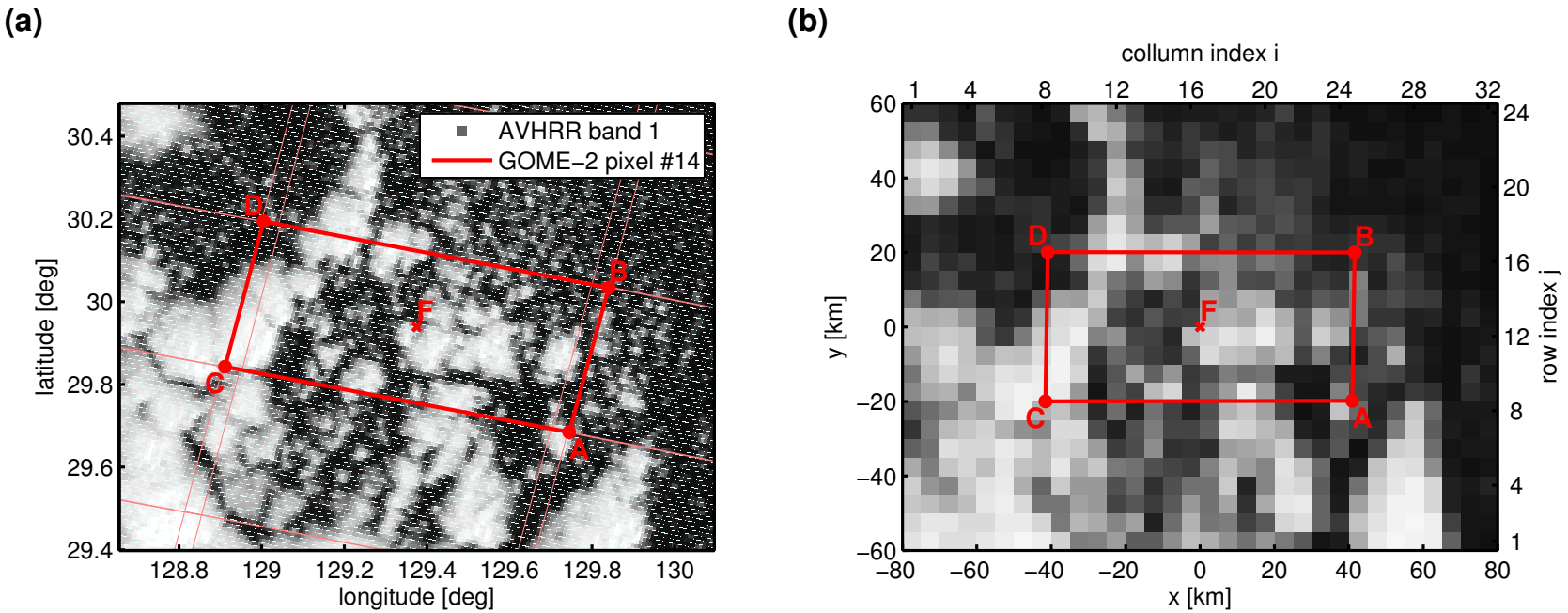

- *from* topocentric (longitude/latitude-plane)
- *to* regularized grid (x/y-plane)
- *via* rotation matrices

Discrete PSF sampling
Equations

One measurement → one equation

$$r = c_0 + \sum_i \sum_j c_{ij} h_{ij} \quad \rightarrow \quad r = c_0 + \sum_{k=1}^{n} c_k h_k$$

r LR radiance

h gridded HR radiances

c PSF parameters

Many measurements → linear equation system

$$\begin{pmatrix} r_1 \\ \vdots \\ r_m \end{pmatrix} = \begin{pmatrix} 1 & h_{11} & \cdots & h_{1n} \\ \vdots & \vdots & & \vdots \\ 1 & h_{m1} & \cdots & h_{mn} \end{pmatrix} \begin{pmatrix} c_0 \\ \vdots \\ c_n \end{pmatrix}$$

- number of measurements $m \approx 100,000$
- number of unknowns $n \approx 1,000$

Definition of pixel numbers

GOME-2 swath

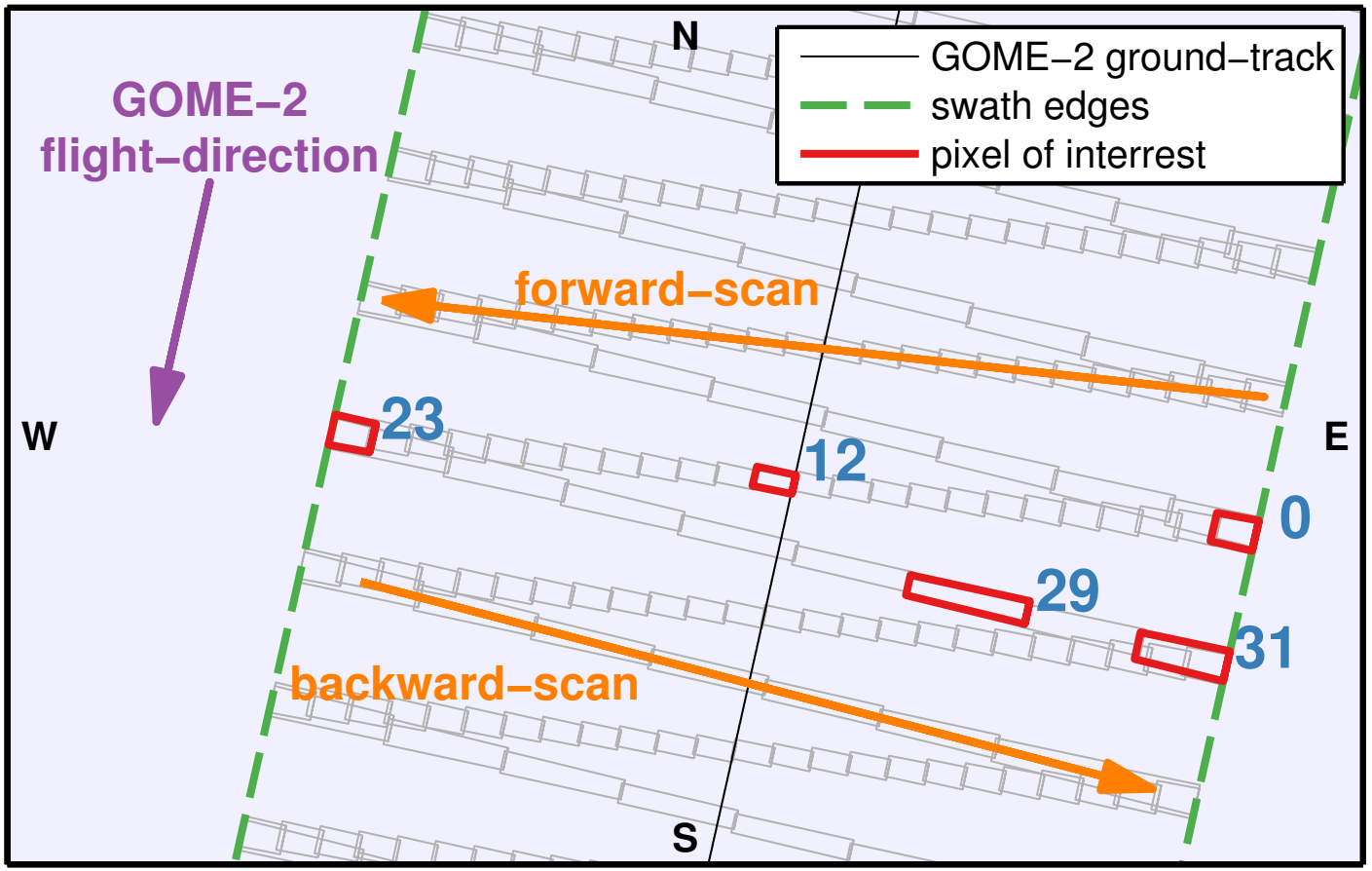

Results

GOME-2 pixel 12 (nadir)

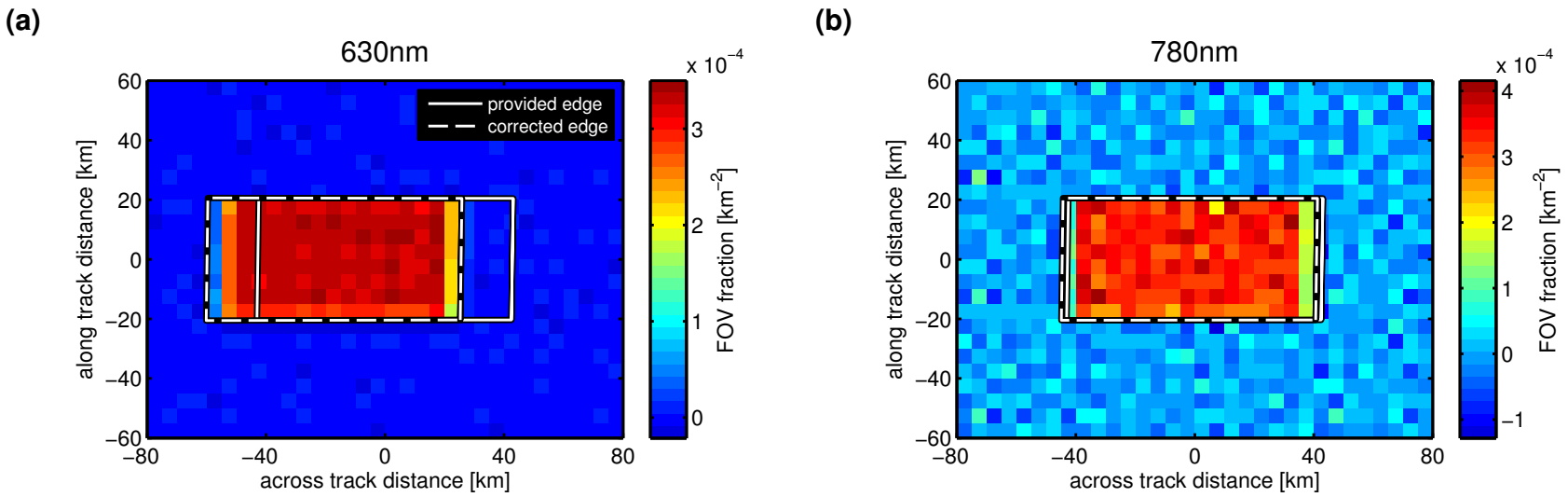

- rectangular FOV shape as provided
- spatial aliasing of pixel edges, depends on LR channel
- applying more distant spectral range increases noise (despite ocean-only red edge filter)

Results

GOME-2 pixel 23 (west) and 0 (east)

pixel 23 – western swath edge

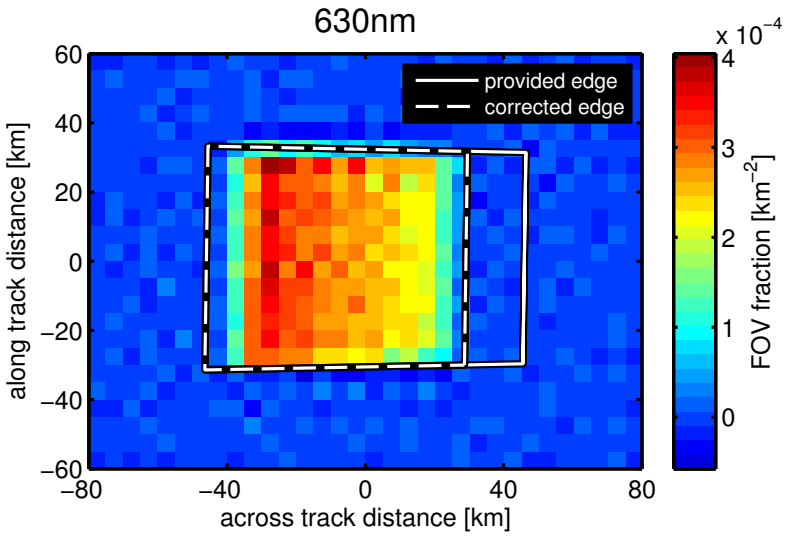

pixel 0 – eastern swath edge

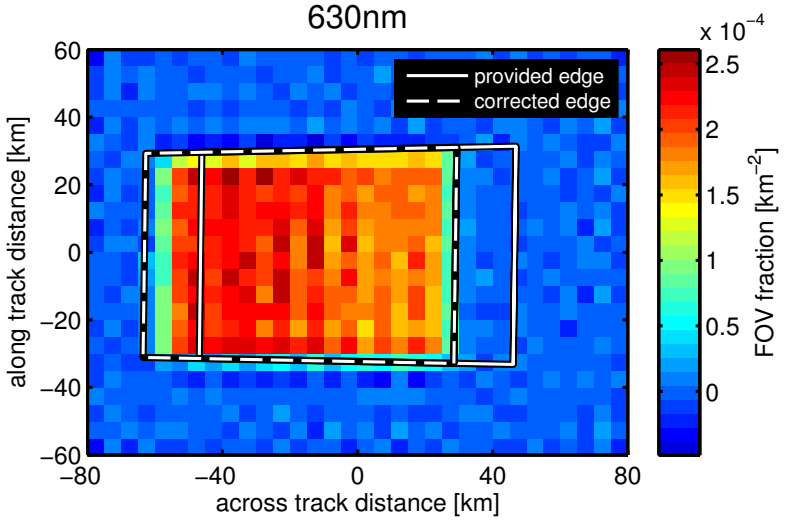

- slightly heterogeneous pattern (AVHRR, scanner motor?)
- scan direction changes in pixel 23

Results

GOME-2 backward-scan pixel 31 (last)

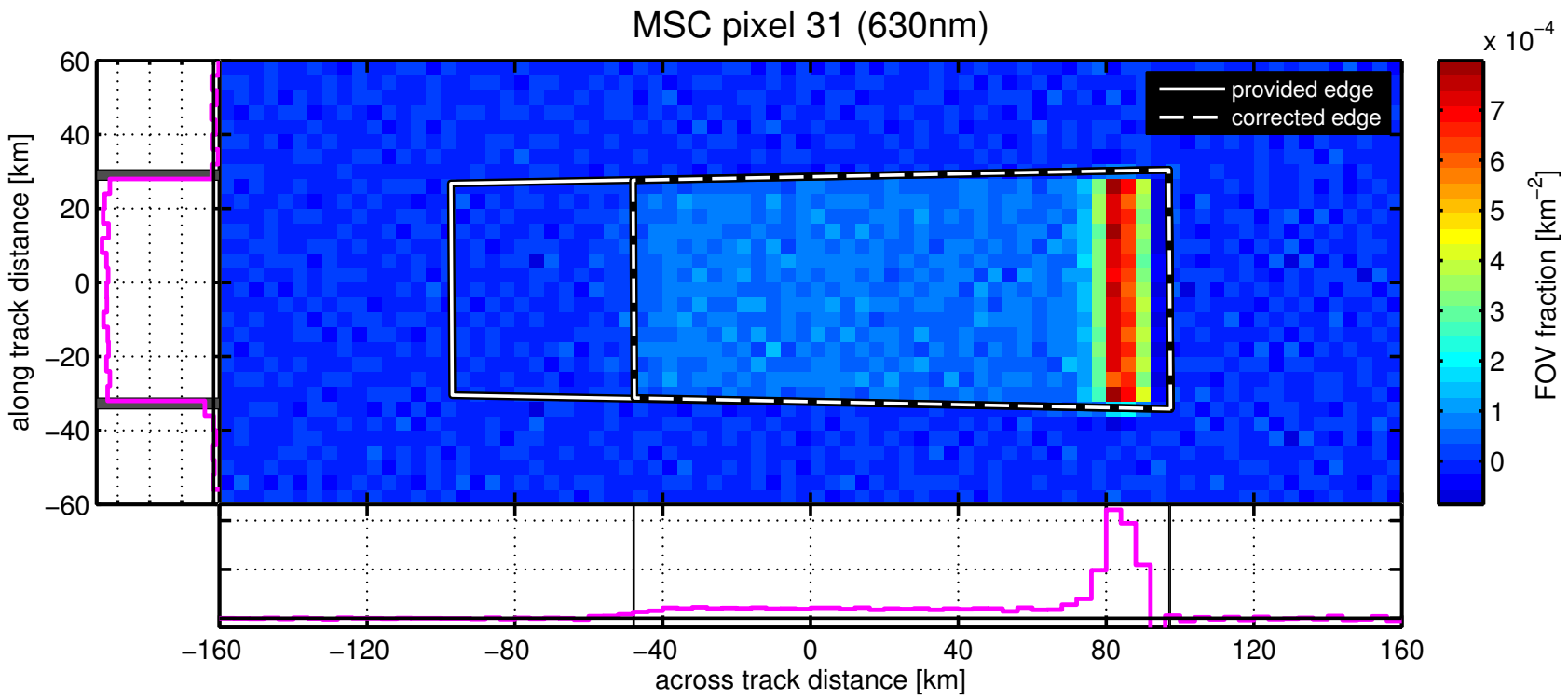

- inhomogeneous FOV due to mirror turn during integration

Results

retrieval error depending on pixel number

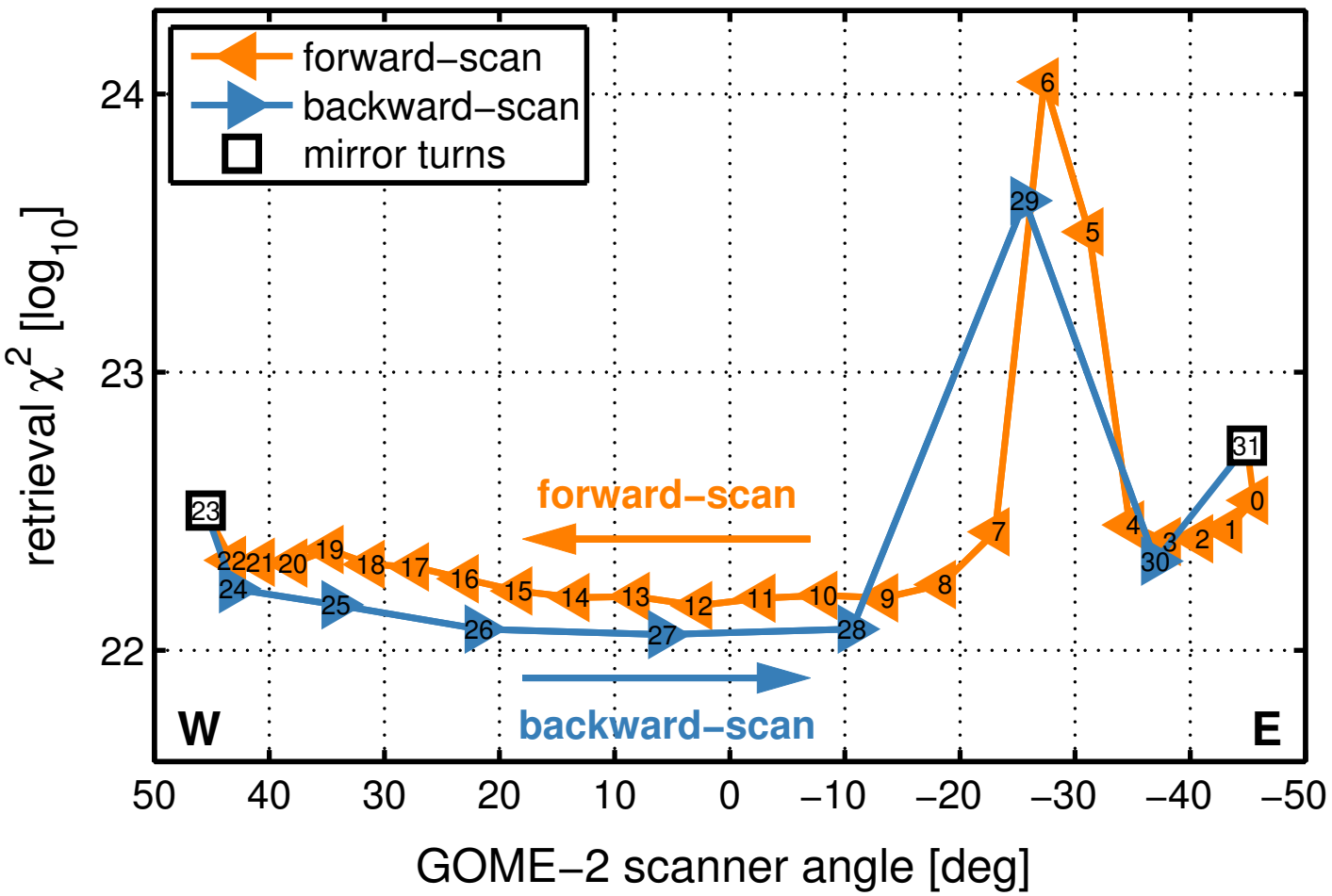

Results

GOME-2 backward-scan pixel 29

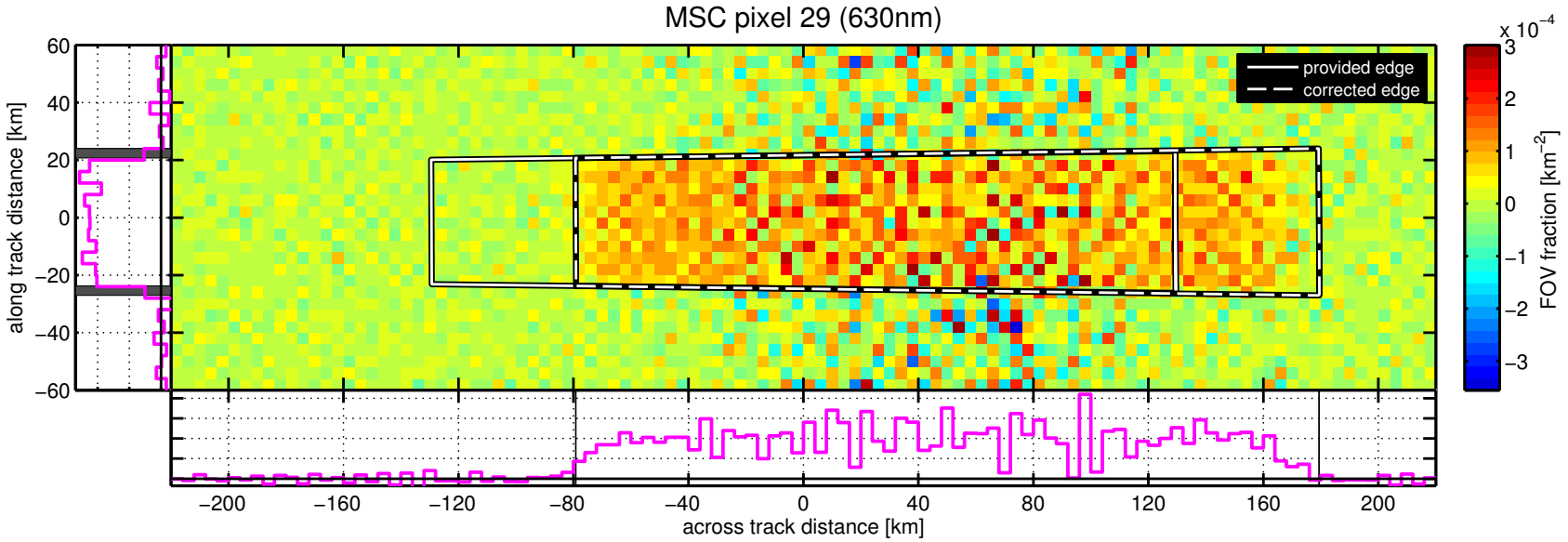

- retrieved FOV noisy due to inaccurate mirror alignment?
- but motor toque profile is ambiguous

Finally: MAX-DOAS

Results from SO_2-camera

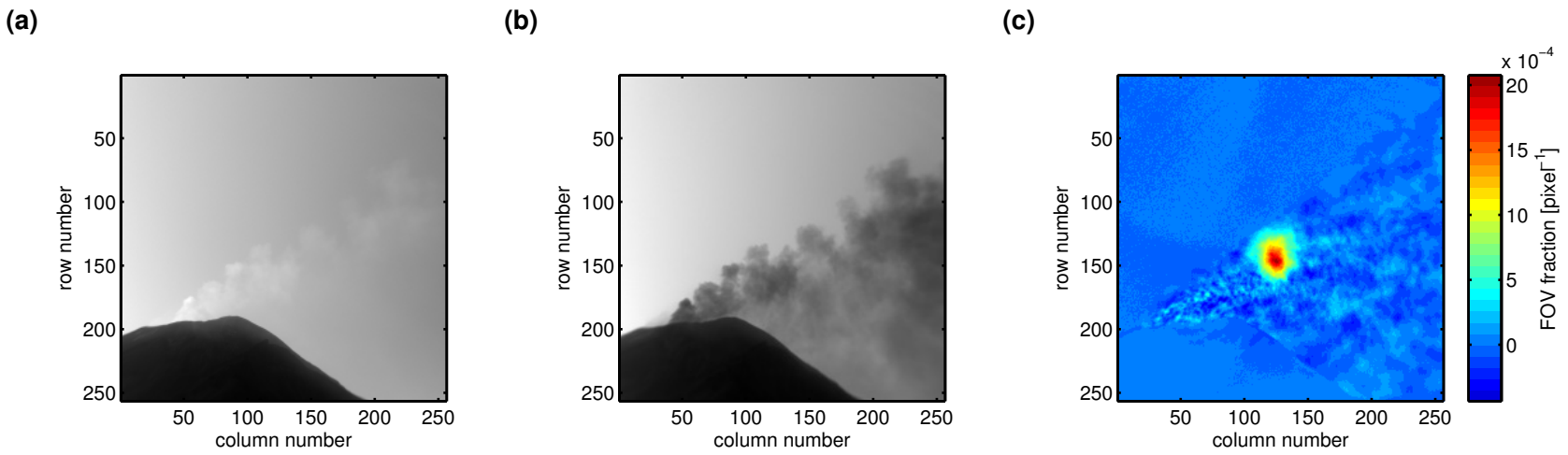

- SO_2-camera vs. MAX-DOAS (NFOV-DOAS)
- measurements at Popocatépetl volcano
- MAX-DOAS instrument alignment changed during transport to field-site

Summary & conclusions

- basic linear model to parametrise LR FOV
- applies correlated HR measurements
- simple/cheap method compared to pre-calibration
- GOME-2
  - provided rectangular FOV reasonable
  - spatial aliasing effect not corrected so far
  - potential scanner misalignment greater than expected
- MAX-DOAS
  - very easy to implement
  - FOV of misaligned telescope reconstruction
  - requires structured and calibrated HR data

Summary & conclusions

- basic linear model to parametrise LR FOV
- applies correlated HR measurements
- simple/cheap method compared to pre-calibration
- GOME-2
  - provided rectangular FOV reasonable
  - spatial aliasing effect not corrected so far
  - potential scanner misalignment greater than expected
- MAX-DOAS
  - very easy to implement
  - FOV of misaligned telescope reconstruction
  - requires structured and calibrated HR data

Thank you for your attention!

Appendix

Discrete PSF sampling
Equations II

Analytical error estimation

- reduced chi-squared

$$\chi^2 = \frac{\|\boldsymbol{I} - \mathbf{H}\boldsymbol{c}\|_2}{m-n} \tag{1}$$

- covariance matrix

$$\Sigma_c = \chi^2 \left(\mathbf{H}^T\mathbf{H}\right)^{-1} \tag{2}$$

- standard deviation of PSF coefficient c_k

$$\sigma_k = \sqrt{(\Sigma_c)_{kk}}$$

Observed error

GOME-2 science channel 4 ↔ AVHRR

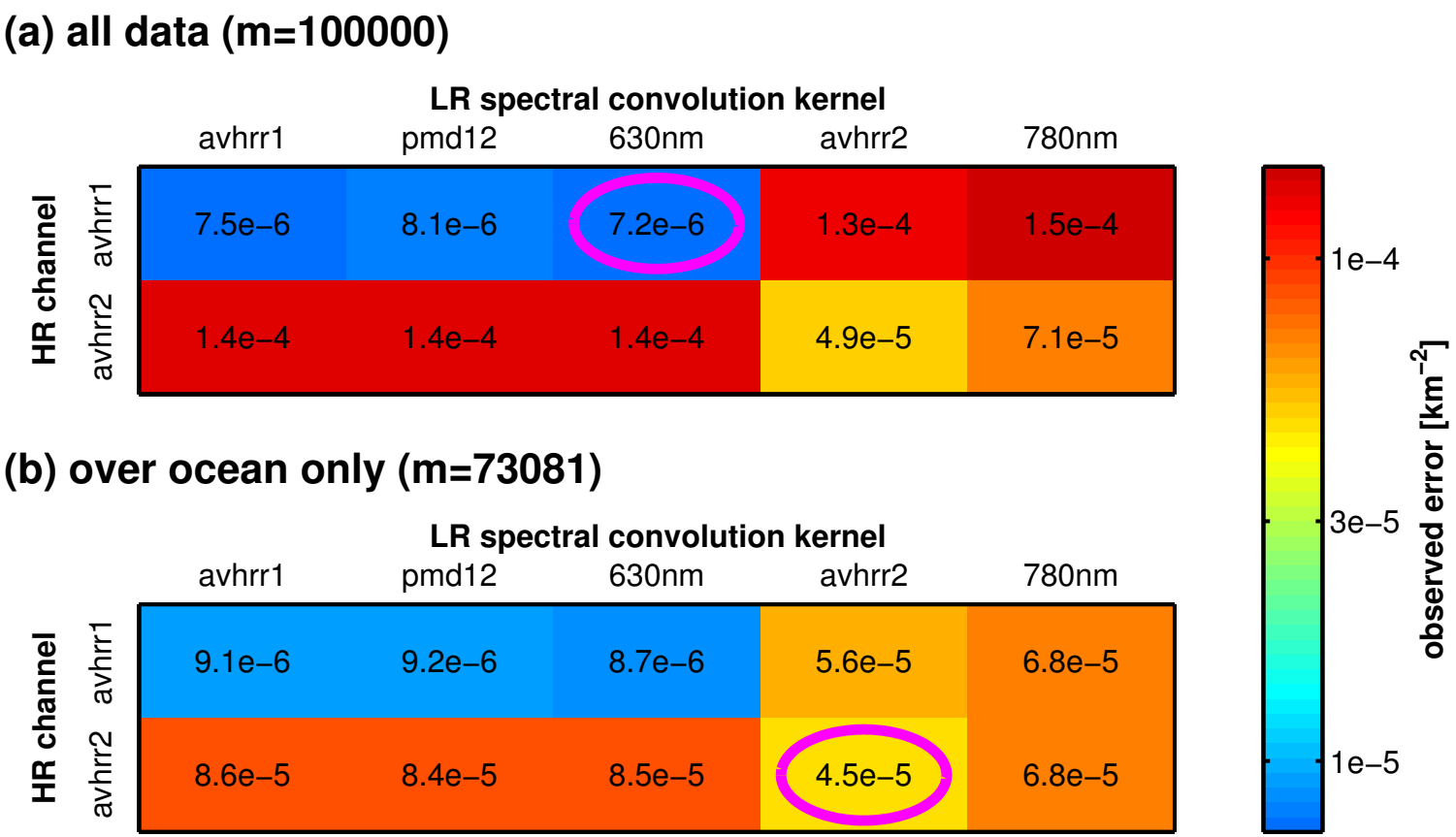

- filter of red-edge influence (over land) improves S/N
- results for red end (beginning of read-out) remain inferior

Estimated error vs. observed error

GOME-2 PMD channel 12 ↔ AVHRR channel 1

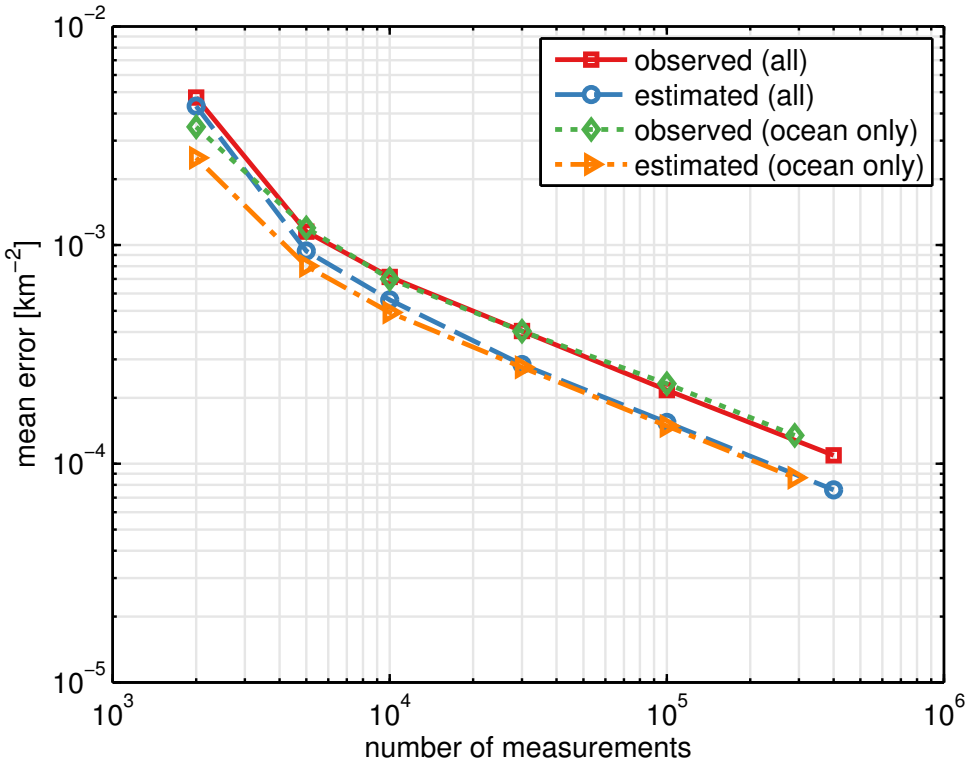

- $\propto m^{-1/2}$ behaviour consistent
- analytically derived error estimates are *too low* ($\approx 25\%$)
- error limit not reached at $m = 400,000$

Results

GOME-2 narrow swath vs. PMD (nadir)

narrow swath 630 nm

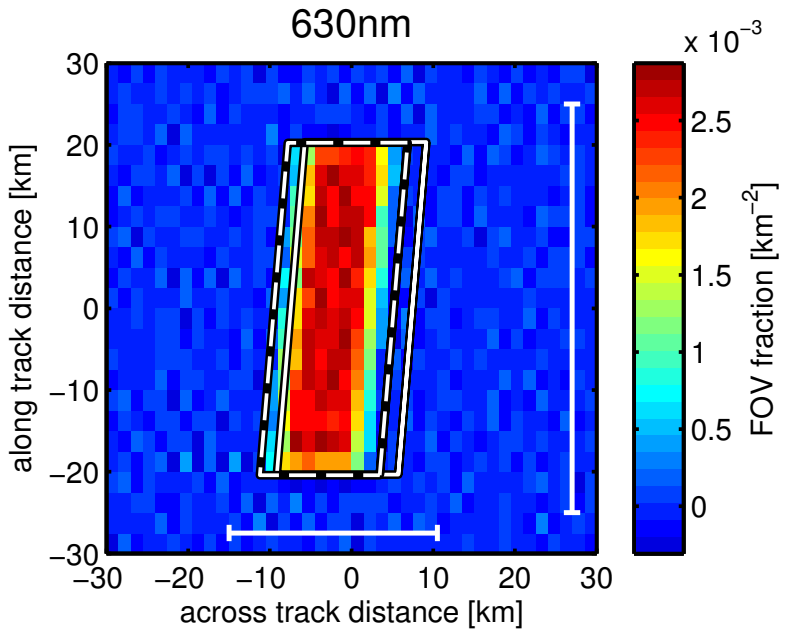

PMD channel 12

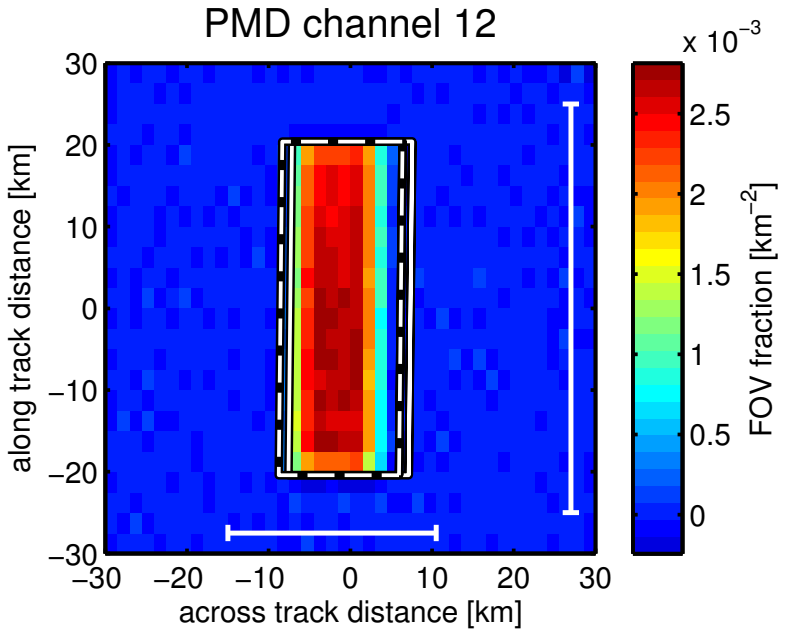

- increased resolution to resolve smaller FOVs
- PMD less tilted due to shorter integration time
- is PMD N/S FOV gradient significant?

What about OMI?

Spectral range of OMI vs. MODIS

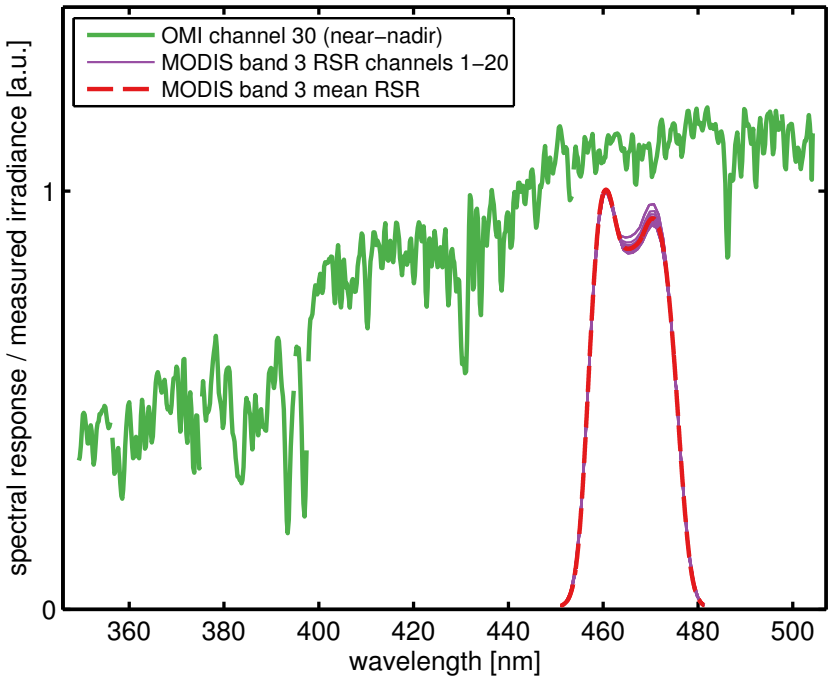

- OMI VIS channel $\leftrightarrow$ MODIS band 3

- 8 min delay between MODIS and OMI measurements
- filter high wind-speed to suppress cloud movement
- exact inversion failed $\rightarrow$ LSMR approximation

Results
OMI pixel 30 (nadir)

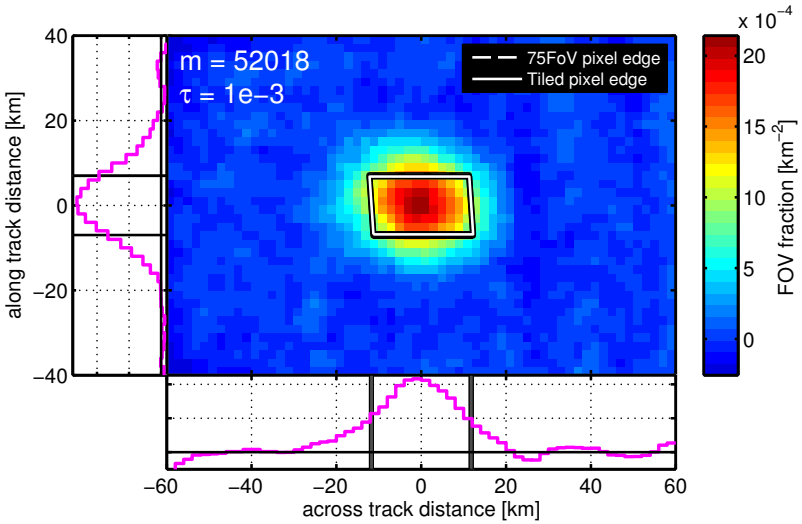

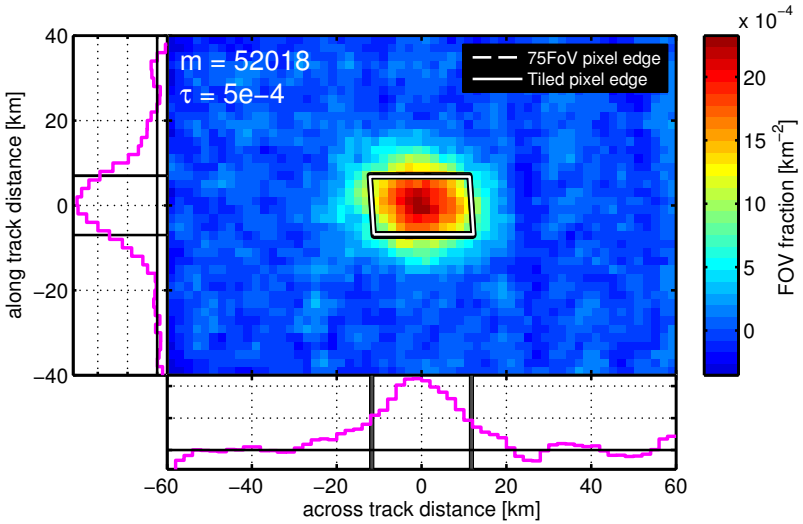

- FOV not as quadrangular than most illustrations suggest
- this is partially documented, but seldom applied

parametrise the observed shape with flat-topped Gaussian

$$F(x,y) = a_0 + a_1 \exp\left[-\left|\frac{x-a_2}{a_3}\right|^{a_4} - \left|\frac{y-a_5}{a_6}\right|^{a_7}\right]$$

Results

OMI pixel 30 (nadir)

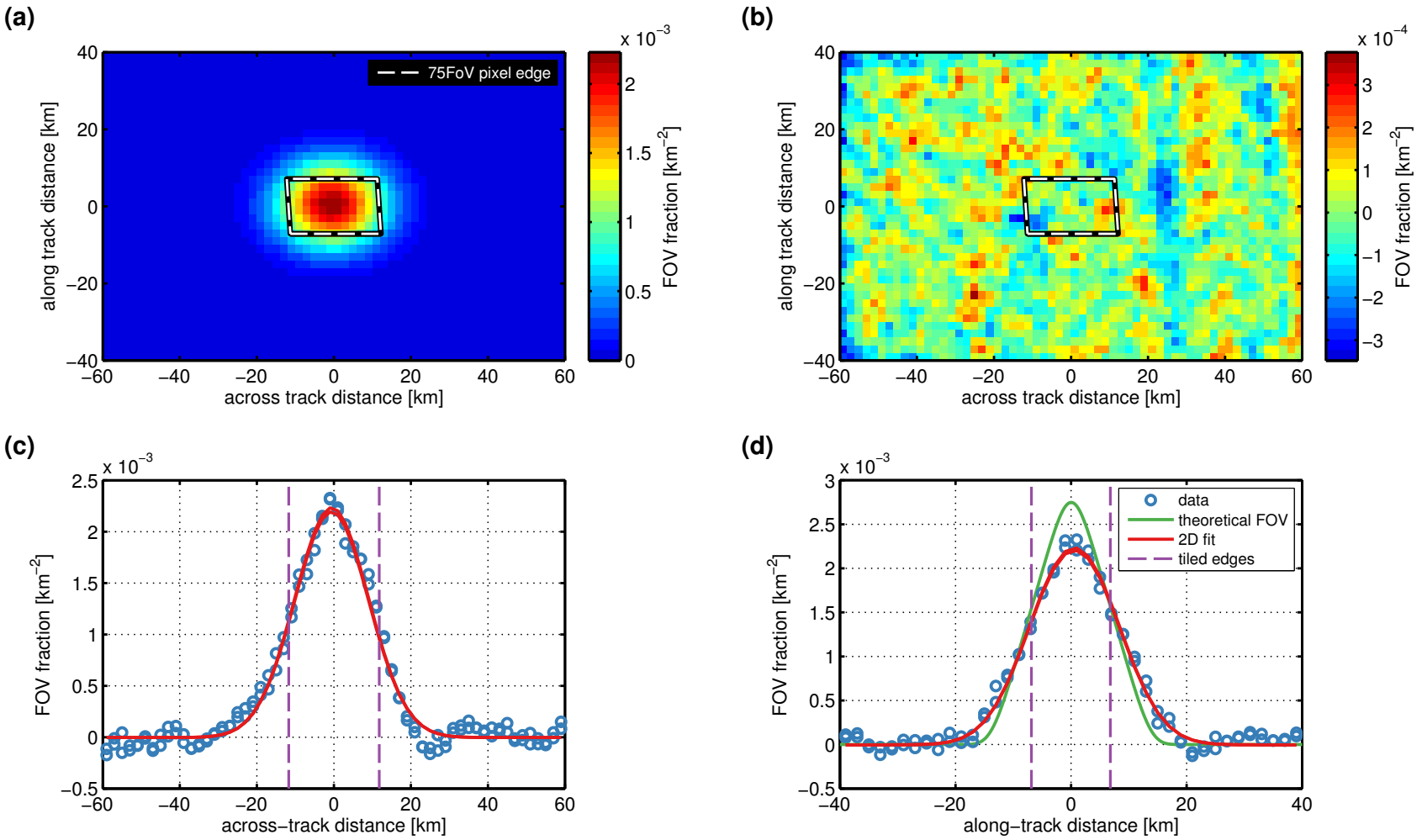

- derived FOV only slightly blurred than prescribed FOV

Results

OMI pixel 05 (western edge of MODIS swath)

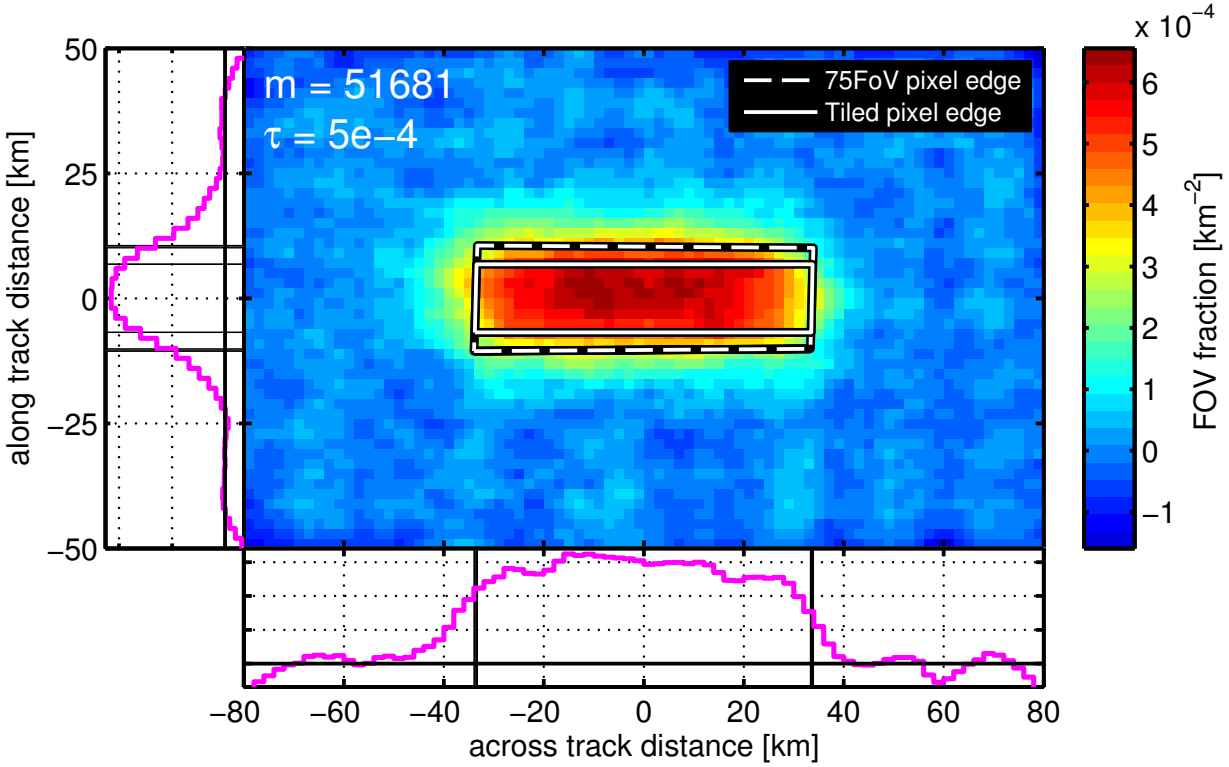

- FOV well constrained by provided edges
- tiled pixel edge inferior than 75FoV pixel edge

Results

OMI pixel 58 (eastern edge of MODIS swath)

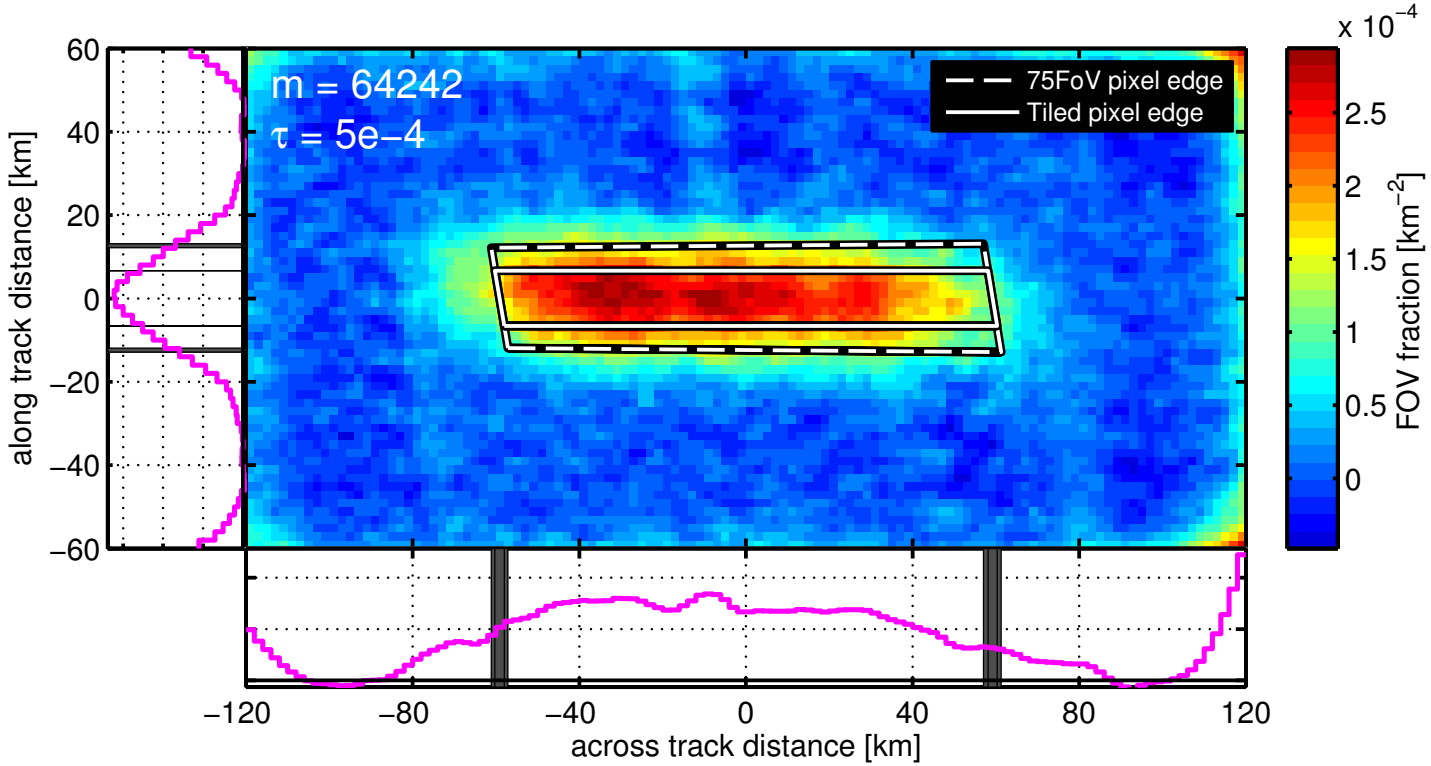

- harmonic artefacts from HR-sampling
- large values at ROI edge indicate systematic errors not captured by the linear model → straylight?

Results

OMI spatial offset depending on pixel number

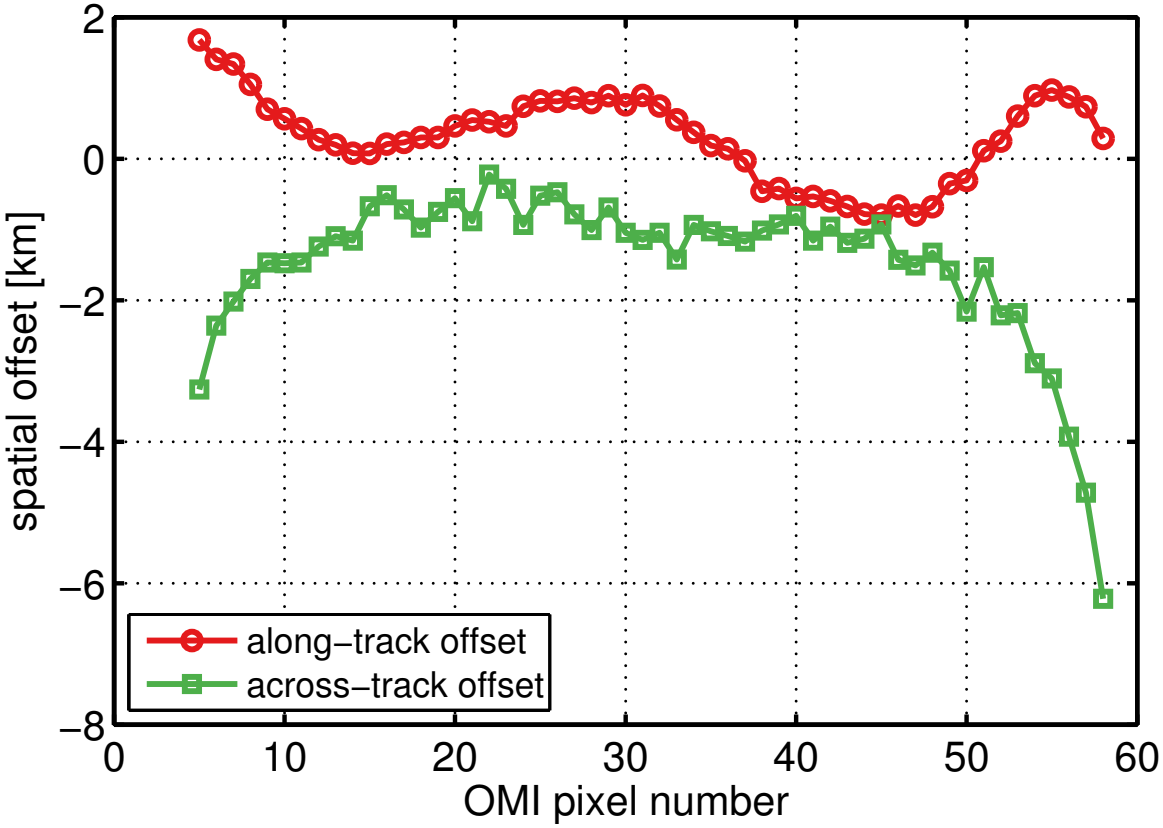

- systematic spatial offset in both directions

→ retrieval bug?

Appendix
OMI row anomaly

- 2007

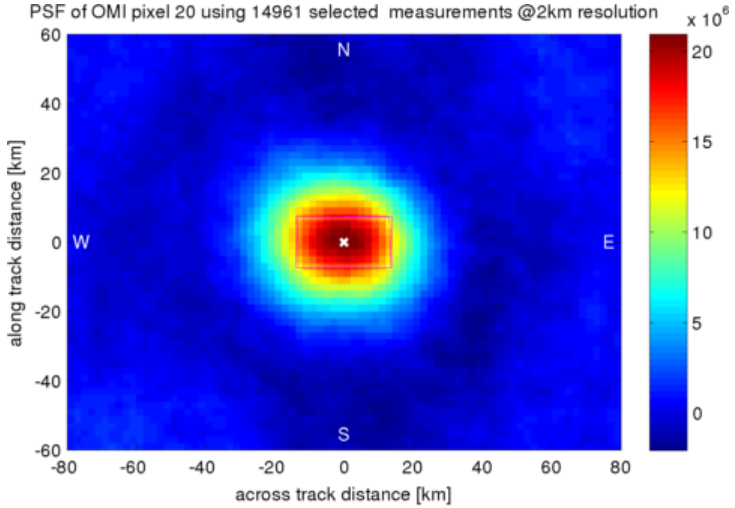

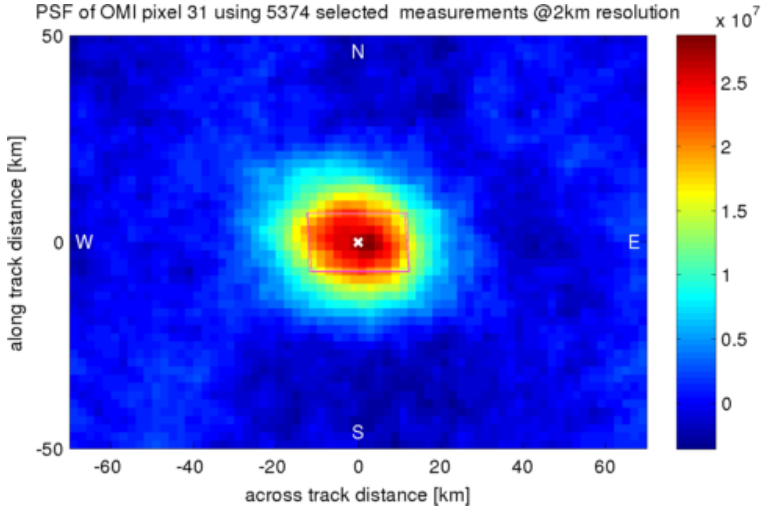

- 2011 (row anomaly)